

Multi-Robot Collaboration for Electronic Textile Fabrication

Danming Wei, *Student Member, IEEE*, Sushmita Challa, Mohammad S. Islam, Jasmin Beharic, Cindy K. Harnett, and Dan O. Popa*, *Senior Member, IEEE*

Abstract— This paper presents a deterministic alignment process of fabric textiles and MEMS clamps. We describe the capability of aligning and fastening textile layers to create electronic textiles using multi-robot collaboration in the NeXus, a custom additive manufacturing robotic system. To complete the alignment process, two industrial robotic arms and one custom positioner were employed. Also, different robotic process tools were used in the alignment and fastening process. A semi-automated interface was programmed and integrated with the robotic tool change process, visual servoing, target detecting, and UV curable adhesive printing functions within the NeXus. The yield of alignment results of the MEMS clamps was assessed, and the completed corresponding fabric intersections were more than 95%.

I. INTRODUCTION

Fiber substrates present unique properties such as permeability, flexibility, conformability, and breathability compared to conventional thin-film substrates on which electronics are generally built. Various methods for manufacturing electronic textiles (E-textiles) are described in the literature, from building functional fiber systems [1, 2] to embedding electronics into 2-D fabric structures [3]. Microelectromechanical systems (MEMS) structures integrated into functional fiber assemblies find applications in textile circuitry [4], wearable sensors [5], switchgear systems [6], and MEMS packaging on flow-through mesh substrates [7]. Functional fiber systems can offer highly conductive electrical fiber traces compared to printed thin films. Ohmic fiber crossovers enable textile circuit routing which can implement fabric-based logic circuits, multiplexers, memory devices, wire electrochemical transistors (WECT) [8], and pressure sensors [9].

Because conventional fiber assemblies are irregular in nature and are subject to distortion, stretching, and shrinking, it makes the process of identifying the functional fiber crossings a laborious task. To keep the fabric structures and fiber crossings at the constant features and locations, we fixed the fabric structures with a 3D printed frame for the 1st generation deterministic alignment process of fabric structures with MEMS clamps [10]. In this 1st generation alignment process, three manual linear stages, two motorized linear stages, and one motorized rotation stage were set up for hardware to complete the alignment process. However, the 3D printed frame was not rigid enough, it had some deformations when it was clamped. Also, the level of the frame was adjusted by manual operation. It was not very precise and repeatable. In addition, because the stages had a limited travel range, the human operator had to adjust the camera to reach different

MEMS clamps locations to check the alignment results, which resulted in more uncertainties in the alignment process. Due to the above disadvantages of the 1st generation alignment process, we developed a 2nd generation alignment process with a multi-robot collaboration including two industrial robotic arms and one custom high-resolution positioner integrated with multiple functions, these functions include a robotic tool change process, visual servoing, target detecting, and UV curable adhesive printing. Also, a metal frame was made to clamp the fabric substrate to secure fibers deterministically and ensure dimensional stability. A corresponding sample chuck was designed to carry a 4-inch wafer placed on the custom positioner. Metalized MEMS clamps fabricated on the 4-inch wafer were to contact conductive fibers toward electronic integration of MEMS with E-textile. The reason to use MEMS clamps rather than adhesives to fix the fabric intersections is due to the desire to not interfere with the surface micromachining release process.

Multi-robot collaboration has been widely applied in many industries, for instance, in vehicle manufacturing to assemble an entire vehicle, and in logistics industries to classify and distribute packages and products to various destinations. Automated guided vehicles' collaboration in robot warehouse systems is often optimized using new methods in path planning and obstacle avoidance [11]. Multi-robot collaboration technology for large-scale additive manufacturing for 3D printing has also been recently researched in [12]. Multi-robot collaboration based on sensing strategies to explore the surrounding environment has been studied in [13].

In this paper, multi-robot collaboration has been employed in the alignment process of a MEMS clamps array with a fiber mesh. Results show that it can improve the precision of the alignment results and enhance the alignment yield by image analysis. The paper is organized in the following orders: Section II presents an electronic textile design; Section III demonstrates a custom robotic system for completing the deterministic alignment process of E-textiles; Section IV details the deterministic alignment process; in Section V, experimental results are presented and discussed; finally, in Section VI, we conclude the paper.

II. ELECTRONIC TEXTILE DESIGN

To fabricate the electronic textile, a novel process was developed to integrate fabric material with MEMS clamps. The fabrication process is described below:

- **Create a fabric sample in Fig. 2(a):** The fabric mesh design consists of 500 to 1000 microns thick non-conductive base fibers arranged in a grid format with the inter-fiber

* Authors are with the Louisville Automation and Robotics Research Institute and Electrical and Computer Engineering Department, University of Louisville, Kentucky, USA (e-mail: danming.wei@louisville.edu).

spacing of 4mm. The design has two 400 to 800 microns thick non-touching parallel conductive fibers which follow a serpentine course along the intersections of the base mesh grid, such that an angle of 45 degrees is formed between the base fiber and the conductive fiber at their intersections. The tolerance of the successful grasp is approximately 1600 microns.

• **Identify the intersections in the fabric in Fig. 2(b):** A binary image processing algorithm was employed in MATLAB® based on the high-resolution image of the framed fabric to identify the intersections in the fabric. The binary image processing algorithm identifies a pattern of pixel distribution around the white pixels (representing the fibers over dark contrast background) to identify the fiber intersections. Sometimes the fiber distortions, and imperfect fiber paths can affect this pixel neighborhood distribution which might not match the predefined intersection pattern within the tolerance range as shown in Fig. 1. This results in false negatives and false positives affecting the efficiency and accuracy of the Algorithm. But the efficiency changes from sample to sample, wherein there were cases where the efficiency went up to 97.8%.

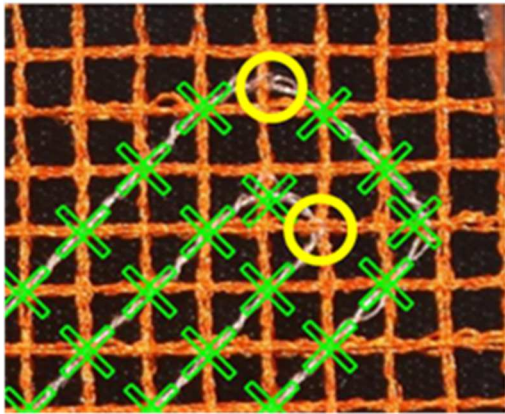


Figure 1. Missed electrical intersections at fiber distorted turnings circled in yellow.

• **Design a MEMS clamps layout in Fig. 2(c):** The MEMS layout design specific to the framed fabric was created in L-edit layout software according to the identified intersections in the fabric. The 12-finger clamp design in Fig. 2(d) consists of T-shaped traces which are aimed to clasp the conductive fibers towards making electrical contact, while the L-Shaped clamp arms clasp the base fiber intersections for mechanical support. The trace lengths are chosen such that reliable scope of the clasp is obtained which further depends on the radius of curvature of the clamp and fiber feature. Otherwise, a specific alignment mark in Fig. 2(f) was added in the MEMS layout to be the specific target in the deterministic alignment process with the visual servoing function.

• **Align the MEMS wafer with the framed fabric:** Instead of using the hardware in the 1st generation alignment process [10], a multi-robot collaboration technique was developed and implemented to complete the 2nd generation deterministic alignment process, which will be detailed in the next sections.

III. NEXUS SYSTEM DESCRIPTION

To develop the 2nd generation deterministic alignment process for MEMS clamps with the framed fabric, the NeXus system was utilized. The NeXus is a custom multiscale additive manufacturing robotic platform with integrated 3D printing techniques and robotic assembly. It is comprised of several subsystems, such as an OPTOMECC® aerosol jetting print station, a stationary 3D printing station, an intense pulse light (IPL) photonic sintering station, a microassembly station, a weaving station, and a tool change station as shown in Fig. 3. Otherwise, the NeXus integrates two industrial robotic arms, a 6-DOF industrial robotic arm, and a 4-DOF industrial robotic arm, to handle and position the material. Also, a custom high-resolution 6-DOF positioner as a carrier with different sample chucks was designed to satisfy different applications.

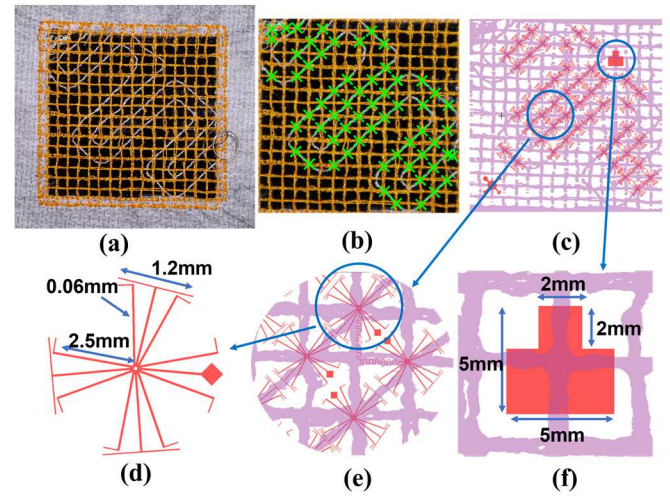


Figure 2. The image of the fabric structure. (b) (c) MEMS clamps and alignment mark distribution for mask design. (d) Single MEMS clamp structure dimension. (e) MEMS clamps align on the intersections of the fabric. (f) Alignment mark dimension.

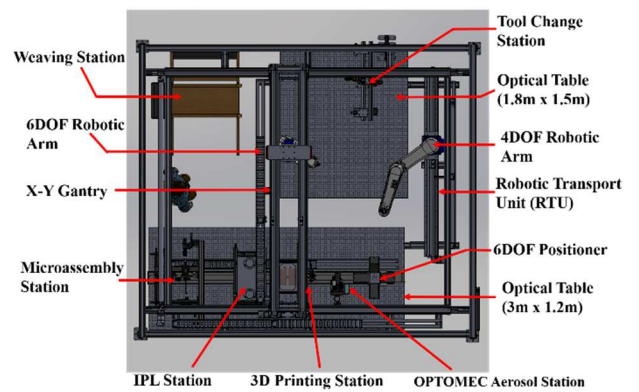


Figure 3. Design of the NeXus system and subsystem distribution.

For deterministic alignment of fabric structure with MEMS clamps, we employed three different robots in the NeXus: the 6-DOF robotic arm, the 4-DOF robotic arm, and the 6-DOF positioner as well as different tools, like HIWIN XEG-32 electrical gripper (HIWIN Corporation, IL, USA) and Nordson EFD794 Auger Valve (Nordson Corporation, OH, USA), on the tool change station. Each robot has specific functions for the deterministic alignment process.

• **6-DOF robotic arm:** it is an industrial robot DENSO VS-6577B (DENSO Corporation, CA, USA), which was ceiling mounted on a large X-Y gantry (Macron Dynamics, Inc., PA, USA) with a 2800mm x 2250mm (X x Y) travel range to maximize the workspace of the 6-DOF robotic arm in the NeXus system. The 6-DOF robotic arm is responsible for picking up the HIWIN electrical gripper on the tool change station to grasp the metal frame clamping the fabric structure in Fig. 4 (a).

• **4-DOF robotic arm:** it is another industrial robot DENSO HM-40A04M (DENSO Corporation, CA, USA), which was mounted on a robotic transport unit (RTU) (Macron Dynamics, Inc., PA, USA) with a 2300mm linear travel range. A Dino-lite camera AM73915MZTL (Dunwell Tech, Inc., CA, USA) was mounted on a 4-DOF robotic arm for detecting targets, like the intersection for the center of the alignment mark and the MEMS clamps to check the alignment results after visual servoing completion. With the feedback of the camera, the alignment mark can be fine-adjusted to match the corresponding intersection on the fabric. Also, the 4-DOF robotic arm needs to pick up the Auger Valve to dispense UV curable adhesive on the fabric to make the wafer stick to the bottom of the fabric.

• **6-DOF positioner:** it is composed of a long coarse linear stage with 2500mm travel (IAI America, Chicago, IL, USA), two fine linear stages (Newport® M-ILS300LM-S), a Z stage (Newport® GTS70VCC), a tilt (T) stage (Newport® BGS80CC) and a rotation (R) stage (Newport® URS50BCC) (Newport® Corporation, CA, USA). Those six motorized stages built up an X-Y-X-Z-T-R, total 6 degrees of freedom, positioner. The 6-DOF positioner can be transferred to different stations along with the IAI stage for specific applications on the long optical table. A 4-inch wafer sample chuck in Fig. 4(b) was designed to couple the metal frame. It was fixed on the top of the 6-DOF positioner by the ATI QC-11 tool change coupler in Fig. 4(c) (ATI Industrial Automation, Inc., NC, USA). The wafer with the MEMS clamps was loaded on the sample chuck and attacked by vacuum.

The evaluation precision of the NeXus was investigated in [14], the precision figures of the merits of the 6-DOF positioner and industrial robotic arms are listed in Table I and Table II.

TABLE I. PRECISION FIGURES OF MERIT OF 6-DOF POSITIONER

	6-DOF Positioner					
	X _L	Y	X	Z	Tilt	Rotation
Travel (mm)	2500	300	300	70	90 deg	360 deg
Accuracy (μm)	-	2.5	2.5	1.75	30mdeg	25mdeg
Repeatability (μm)	17	5	5	0.5	2.5mdeg	1mdeg
Resolution (μm)	10	0.01	0.01	0.25	0.2mdeg	0.5mdeg

TABLE II. PRECISION FIGURES OF MERIT OF INDUSTRIAL ROBOTS

	Accuracy (μm)	Repeatability (μm)
<i>6-DOF robotic arm and X-Y gantry</i>		
X-Y gantry	10.8	22.7
6-DOF robotic arm	15.3	11.0
Combination	15.6	34.7
<i>4-DOF robotic arm and RTU</i>		
RTU	16.7	22.5
4-DOF robotic arm	4.0	8.2
Combination	18.6	28.6

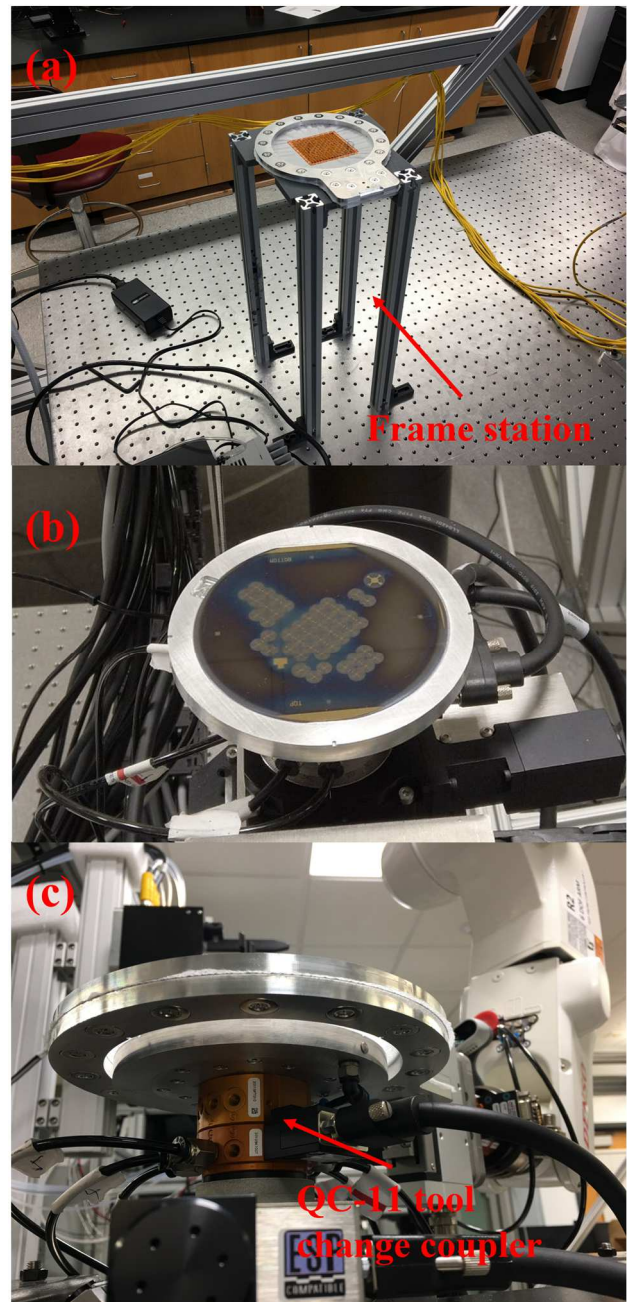


Figure 4. Metal frame clamping fabric material on the standing; (b) 4-inch wafer sample chuck carrying the wafer with MEMS clamps; (c) Metal frame coupling with 4-inch wafer sample chuck.

IV. DETERMINISTIC ALIGNMENT PROCESS

The deterministic alignment of fabric structure with MEMS clamps is a process of three-robot collaboration depicted in Fig. 5 and implemented in Fig. 6. To carry out the process, a sequence of automated robot operation steps was formulated and implemented in our robot controller, including sample loading, robotic tool change process, visual servoing, and UV curable adhesive dispensing. A complete description of these steps is listed below:

1. The 4-inch wafer sample chuck needs to be placed on the 6-DOF positioner, then needs to load the 4-inch wafer with the fabricated MEMS clamps on the chuck and turn on the vacuum to attach the wafer.

2. Load the frame that clamps the fabric material on the specific frame station in Fig. 4(a). The metal frame has two pieces of metal plate inserted with several magnets to clamp the fabric sample by magnetic force.

3. Initialize the 6-DOF positioner and then rotate the sample chuck in a 45-degree orientation. Then, initialize two robotic arms at the rest positions, respectively.

4. The 6-DOF robotic arm moves to the tool change station to pick up HIWIN electrical clamps by QC-11 tool change coupler and moves to grasp the fabric frame, then moves the frame above the 4-inch wafer sample chuck.

5. The 4-DOF robotic arm moves to the fabric frame and adjusts the Dino-lite camera above the fabric to focus on the intersection which is for the alignment mark on the wafer. The coordinate of the intersection can be acquired by the MEMS layout design. When the intersection is moved into the camera's field of view, the coordinate and orientation of the intersection can be recorded from the image of the camera.

6. Remove the fabric frame from the top of the wafer and adjust the height of the camera to focus on the alignment mark on the wafer. At this moment, the alignment mark should have some offsets due to errors in loading the wafer on the sample chuck and the frame on the frame station as well as the repeatability and accuracy of the 6-DOF robotic arm and the 6-DOF positioner.

7. Due to the offsets of the alignment mark on the wafer, the visual servoing function was implemented to fine adjust the center of the alignment mark to match the coordinate and orientation of the intersection.

8. When the visual servoing process is completed, the metal frame is moved back to the previous position, thus the center of the alignment mark should match its corresponding intersection. In the vertical direction, the wafer is moved up by the Z stage of the 6-DOF positioner to gently touch the bottom of the fabric material.

9. Adjust the camera to check how MEMS clamps align their specific intersections referred to the coordinate of the center of each MEMS clamp acquired from the MEMS layout design. If the alignment results are not acceptable, repeat steps from 6 to 8. Note that before repeating step 6, the wafer needs to move down back to the initial height to avoid crashes during removing the fabric frame from the top of the wafer.

10. Assuming that the alignment results are acceptable, the 4-DOF robotic arm moves to the tool change station to pick up the Auger valve and then moves back to the 6-DOF positioner and adjusts the nozzle above the fabric by about 1mm distance.

11. Control the Auger valve to dispense UV curable adhesive on the fabric edges following a square pattern with G-code commands.

12. Remove the Auger valve and place it back on the tool change station. Then turn on UV light to cure the UV curable adhesive for at least 10 minutes.

13. Turn off the UV light and the vacuum of the sample chuck and move down the sample chuck. At this moment, the wafer should be stuck on the bottom of the fabric material with the cured UV adhesive.

14. Move the fabric frame back to the frame station. Open the electrical gripper to release the frame. Then place the electrical gripper back in the tool change station. All three robots are reset to their initial positions.

V. EXPERIMENTAL RESULTS

During the deterministic alignment process with the multi-robot collaboration, several significant functions were implemented, such as robotic tool change process, visual servoing, target detecting, and UV curable adhesive printing.

A. Robotic Tool Change Process

There are two tools on the tool changer station in NeXus employed in the alignment process, HIWIN electrical gripper and Nordson Auger valve. The tools were picked up by the 6-DOF robotic arm and the 4-DOF robotic arm respectively using the ATI QC-11 tool change coupler. An electrical gripper was used for grasping the metal frame and holding it parallel with the 4-inch wafer sample chuck. The Auger valve was used for dispensing Dymax 9-20558-REV-A UV curable adhesive (Dymax Corporation, CT, USA) on the fabric material to stick it to the wafer after the alignment process. When the alignment process was done, both tools were placed back in the tool change station at their constant locations.

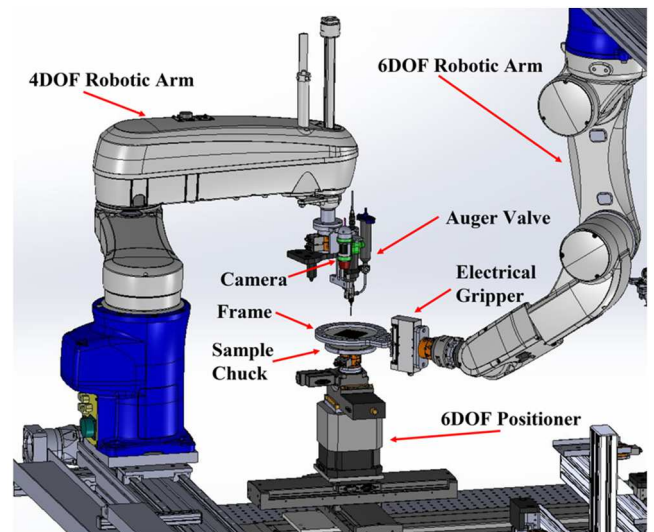


Figure 5. Design of the NeXus system manipulators for fiber and MEMS clamps handling and alignment.

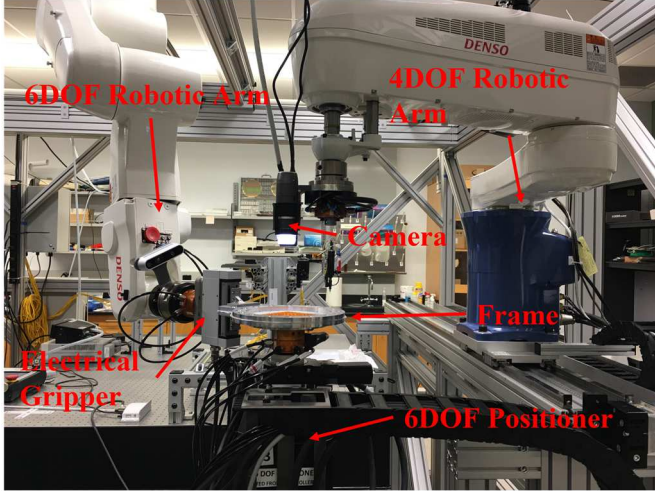


Figure 6. An image of the NeXus system in our lab.

B. Visual Servoing and Target Detection

With the visual feedback of the Dino-lite® camera on the 4-DOF robotic arm, targets, like the intersection for alignment and the MEMS clamps alignment results, can be detected and checked. Also, to improve the precision of alignment results, a visual servoing function was adopted to enhance the accuracy of the alignment between the fabric intersection and the alignment mark. In the visual servoing function, image Jacobian was employed to adjust the center of the alignment mark reaching its corresponding intersection on the fabric based on the coordinate and orientation of the intersection in the image. Equation (1), (2), and (3) [15] expresses how to calculate the motion of stages of the 6-DOF positioner to move the alignment mark to reach its corresponding intersection on the fabric.

$$\begin{bmatrix} \Delta P_x \\ \Delta P_y \\ \Delta P_z \end{bmatrix} = J_{image} \begin{bmatrix} \Delta X \\ \Delta Y \\ \Delta \theta \end{bmatrix} \quad (1)$$

$$J_{image} = \begin{bmatrix} J_{11} & J_{12} & J_{13} \\ J_{21} & J_{22} & J_{23} \\ J_{31} & J_{32} & J_{33} \end{bmatrix} \quad (2)$$

$$\begin{bmatrix} X_{new} - X_{cur} \\ Y_{new} - Y_{cur} \\ \theta_{new} - \theta_{cur} \end{bmatrix} = \Delta s J_{image}^{-1} \begin{bmatrix} P_{x_d} - P_{x_{cur}} \\ P_{y_d} - P_{y_{cur}} \\ P_{\theta_d} - P_{\theta_{cur}} \end{bmatrix} \quad (3)$$

$$J_{image} = \begin{bmatrix} -0.0051597 & 0.0050213 & -0.0337985 \\ 0.00514525 & 0.00557106 & -0.416211 \\ 0 & 0 & -1 \end{bmatrix} \quad (4)$$

where ΔX , ΔY , and $\Delta \theta$ are the variations of the 6-DOF positioner in a plane; ΔP_x , ΔP_y , and ΔP_θ are variations in pixel of the target's center in the Dino-lite camera's field of view. Since the image Jacobian is a 3 x 3 matrix that has 9 entries, the linear least squares estimation method was applied to find the entries' values of the image Jacobian. X_{cur} , Y_{cur} , θ_{cur} , X_{new} , Y_{new} , and θ_{new} are the current and new configuration of the 6-DOF positioner; P_{x_d} , P_{y_d} , P_{θ_d} , $P_{x_{cur}}$, $P_{y_{cur}}$, and $P_{\theta_{cur}}$ are values in pixel of the desired and current position and orientation of the center of the alignment mark in the Dino-lite camera's FOV, Δs represents a step size of the stages' movements. Based on the vision feedback values, the

alignment mark can move to the corresponding intersection in a fast and precise method by using the visual servoing technique in Fig. 7.

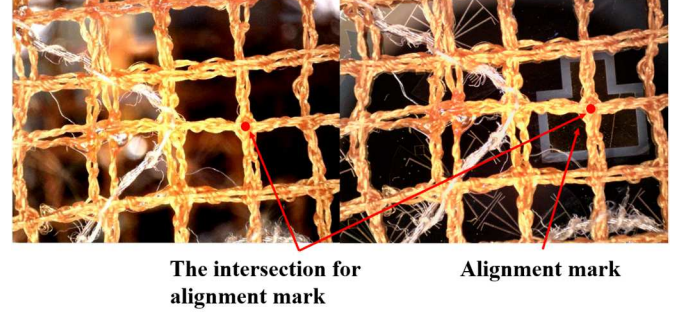


Figure 7. The alignment mark aligns with the specific intersection after the visual servoing process.

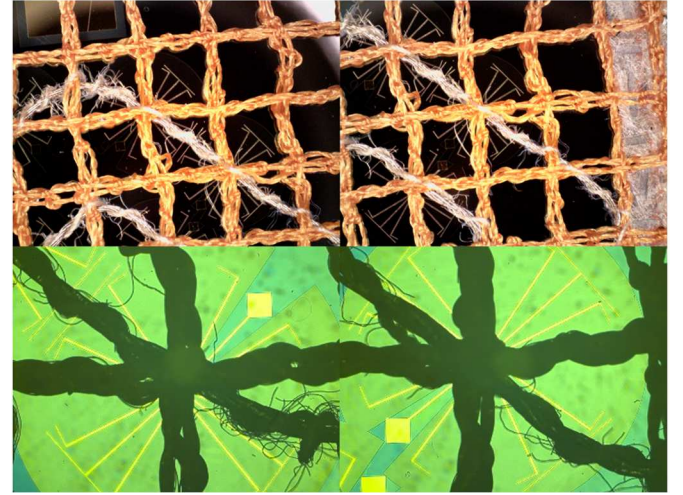


Figure 8. Alignment results of MEMS clamps with fabric intersections.

After the alignment mark on the wafer was aligned with the intersection on the fabric, the Dino-lite® camera was controlled to check random MEMS clamps' alignment results. Fig. 8 depicts some MEMS clamps aligned with their corresponding intersections. Compared with the layout design of the mask for the MEMS clamps fabrication in Fig. 2, after the alignment process with the multi-robot collaboration in the NeXus, the center of each MEMS clamp was aligned with its corresponding intersection properly, which matched the yield in the layout design. The yield of alignment results was more than 95%.

C. Auger Valve Printing

When the alignment process was done, the 4-DOF robotic arm moved to pick up the Auger valve on the tool change station, the DYMAX® UV curable adhesive was set up on the Auger valve, and a gauge-14 nozzle was mounted on the bottom of the Auger valve. The nozzle position was calibrated with respect to the center of the Dino-lite camera. Based on the coordinate of the alignment mark intersection in the image of the camera, the center coordinate of the fabric can be calculated with respect to the center of the camera. The nozzle can be homogeneously transformed to the center of the fabric (shown in Fig. 9) to start the UV curable adhesive printing referred to the G-code generated by Inkscape® software. There was a 55mm x 55mm square pattern of UV curable adhesive was

printed along the outline of the fabric. Then the Auger valve was removed from the top of the frame, the UV light was turned on for at least 10 minutes to cure the UV adhesive.

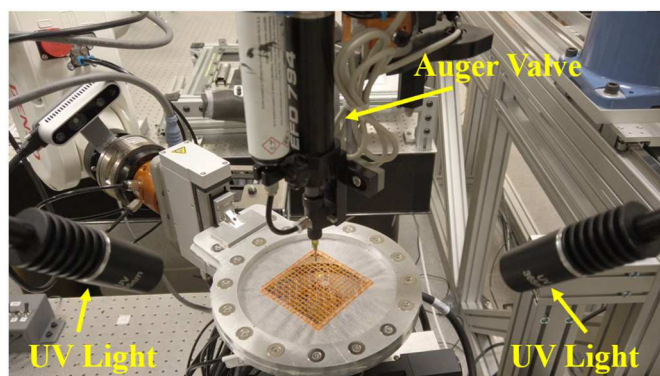


Figure 9. The Auger valve dispenses the UV curable adhesive on the fabric.

D. MEMS Clamps Release Process

When the UV adhesive was cured thoroughly, the wafer was attached to the fabric stably. The fabric with wafer was transferred to the cleanroom to use XeF₂ gas (Xactix, Inc.) to isotropically etch silicon to release the clamp structures. The MEMS clamps pop to grasp the textiles and conductive fibers as shown in Fig. 10. Their purpose is to provide mechanical stability and electrical contact for MEMS devices tethered to functional fibers in a textile.

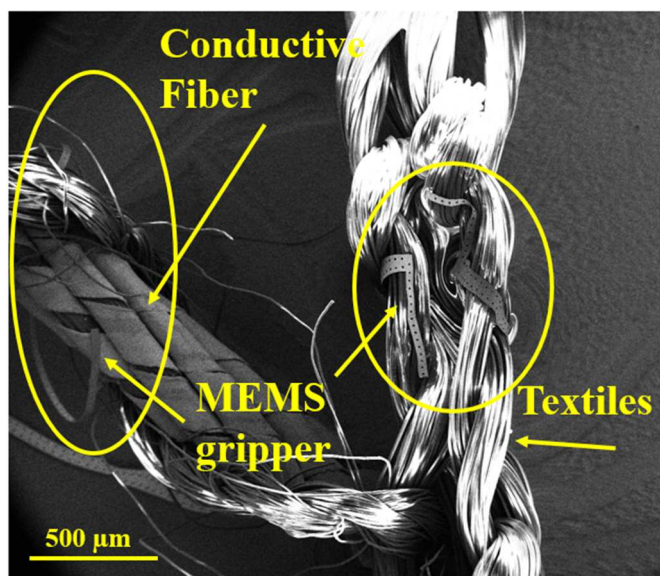


Figure 10. Released MEMS clamps grasp the conductive wire and fabric.

VI. CONCLUSION

A multi-robot collaboration was employed to complete an electronic textile deterministic alignment process. Compared with the 1st generation alignment process, in the 2nd generation alignment process, a metal frame was designed to clamp the fabric material to secure fibers deterministically and ensure dimensional stability, and a 4-inch wafer sample chuck was made to carry the wafer with the MEMS structures. Otherwise, two industrial robotic arms and a custom positioner as well as different tools, like A Dino-lite® camera, an electrical gripper, and an Auger valve, were employed to accomplish the alignment process with high precision and repeatability. The

yield of alignment results of the MEMS clamps and the corresponding fabric intersections are more than 95%. Future work for the automated NeXus manufacturing system could include functional testing of individual devices using the known device locations.

ACKNOWLEDGMENT

This work was supported by National Science Foundation awards MRI #1828355 and EPSCOR #1849213. We would like to thank the help from Chuang Qu and the staff of the Micro and Nano Technology Center at the University of Louisville.

REFERENCES

- [1] Y. Dong, Y. Zou, J. Song, Z. Zhu, J. Li, and H. Zeng, "Self-powered fiber-shaped wearable omnidirectional photodetectors," *Nano Energy*, vol. 30, pp. 173-179, 2016.
- [2] T. L. Buckner and R. Kramer-Bottiglio, "Functional fibers for robotic fabrics," *Multifunctional Materials*, vol. 1, no. 1, p. 012001, 2018.
- [3] K. N. Kim *et al.*, "Highly stretchable 2D fabrics for wearable triboelectric nanogenerator under harsh environments," *ACS nano*, vol. 9, no. 6, pp. 6394-6400, 2015.
- [4] T. Agcayazi, K. Chatterjee, A. Bozkurt, and T. K. Ghosh, "Flexible interconnects for electronic textiles," *Advanced Materials Technologies*, vol. 3, no. 10, p. 1700277, 2018.
- [5] J. Ou, D. Oran, D. D. Haddad, J. Paradiso, and H. Ishii, "SensorKnit: architecting textile sensors with machine knitting," *3D Printing and Additive Manufacturing*, vol. 6, no. 1, pp. 1-11, 2019.
- [6] K. Niayesh, L. Niemeyer, and J. Fabian, "Matrix combination of elementary switches: general considerations and application to MEMS relays," *Electrical Engineering*, vol. 90, no. 1, pp. 19-31, 2007.
- [7] M.-N. Nashed, D. A. Hardy, T. Hughes-Riley, and T. Dias, "A novel method for embedding semiconductor dies within textile yarn to create electronic textiles," *Fibers*, vol. 7, no. 2, p. 12, 2019.
- [8] R. E. Owyung, T. Terse-Thakoor, H. Rezaei Nejad, M. J. Panzer, and S. R. Sonkusale, "Highly flexible transistor threads for all-thread based integrated circuits and multiplexed diagnostics," *ACS applied materials & interfaces*, vol. 11, no. 34, pp. 31096-31104, 2019.
- [9] L. M. Castano and A. B. Flatau, "Smart fabric sensors and e-textile technologies: a review," *Smart Materials and structures*, vol. 23, no. 5, p. 053001, 2014.
- [10] S. Challa, M. S. Islam, D. Wei, J. Beharic, D. O. Popa, and C. Harnett, "Functional Fiber Junctions for Circuit Routing in E-Textiles: Deterministic Alignment of MEMS Layout With Fabric Structure," in *International Manufacturing Science and Engineering Conference*, 2021, vol. 85079: American Society of Mechanical Engineers, p. V002T08A009.
- [11] N. Pinkam, F. Bonnet, and N. Y. Chong, "Robot collaboration in warehouse," in *2016 16th International Conference on Control, Automation and Systems (ICCAS)*, 2016: IEEE, pp. 269-272.
- [12] H. Shen, L. Pan, and J. Qian, "Research on large-scale additive manufacturing based on multi-robot collaboration technology," *Additive Manufacturing*, vol. 30, p. 100906, 2019.
- [13] I. Rekleitis, G. Dudek, and E. Miliotis, "Multi-robot collaboration for robust exploration," *Annals of Mathematics and Artificial Intelligence*, vol. 31, no. 1, pp. 7-40, 2001.
- [14] D. Wei *et al.*, "Precision Evaluation of NeXus, a Custom Multi-Robot System for Microsystem Integration," in *International Manufacturing Science and Engineering Conference*, 2021, vol. 85079: American Society of Mechanical Engineers, p. V002T07A008.
- [15] D. Wei, M. B. Hall, A. Sherehly, and D. O. Popa, "Design and Evaluation of Human-Machine Interface for NEXUS: A Custom Microassembly System," *Journal of Micro-and Nano-Manufacturing*, vol. 8, no. 4, p. 041011, 2020.